

# Photosensitization of Imidazole Derivative by ZnO Nanoparticle

Chockalingam Karunakaran ·  
Jayaraman Jayabharathi · Kumar Brindha Devi ·  
Karunamoorthy Jayamoorthy

Received: 3 November 2011 / Accepted: 7 March 2012 / Published online: 21 March 2012  
© Springer Science+Business Media, LLC 2012

**Abstract** A sensitive imidazole based fluorescent sensor like 4, 5-diphenyl-2(E)-styryl-1H-imidazole, for ZnO has been designed and synthesized via simple steps. The absorption, fluorescence, SEM, EDX and IR studies indicate that imidazole derivative is bound on the surface of ZnO semiconductor. Based on photo-induced electron transfer (PET) mechanism, fluorescent enhancement has been explained and apparent binding constant has been calculated. Ligand adsorption on ZnO nanoparticle lowers of the HOMO and LUMO energy levels of imidazole derivative and the chemical affinity between the nitrogen atom of the imidazole and zinc ion on the surface of the nano oxide may be a reason for strong adsorption of the ligand on nanoparticle. The electron injection from photo excited imidazole derivative to the ZnO conduction band ( $S^* \rightarrow S^+ + e_{CB}^-$ ) accounts for the enhanced fluorescence.

**Keywords** Imidazole · Nanoparticles · Electron transfer · Enhancement · Association constant

## Introduction

Semiconductor nanoparticles attract considerable attention owing to their unique size dependent optical and electronic properties [1, 2] and these materials find potential biotechnological applications like luminescence tagging, immunoassay, drug delivery and cellular imaging [3–5]. ZnO is a fluorescent semiconductor material, the nanocrystals exhibit better

chemical stability and safety relative to other toxic semiconductor nanocrystals. Thus, fluorescent ZnO nanocrystals have become a bio friendly candidate for biological technology application [6, 7]. Unique ZnO nanorods substrate has been grown to immobilize a large amount of probe molecules and also to directly amplify the microarray fluorescent signals in detection of two important cancer biomarkers, carcinoembryonic antigen (CEA) and  $\alpha$ -fetoprotein (AFP), achieving a detection limit of  $1 \text{ pg L}^{-1}$  in human serum, which is comparative to or lower than that of ELISA [8]. Arylimidazole derivatives play important role in materials science due to their optoelectronic properties [9–12]. They are used as ligands for the synthesis of metal complexes of ruthenium (II), copper(II), cobalt(II), nickel(II), manganese(II), iridium (III) and several lanthanides for nonlinear optical (NLO) applications. The reported visible light excited  $\text{Zn}^{2+}$  fluorescent sensors are mainly derived from bulk xanthenone fluorophores, like fluorescein and rhodamine [13, 14]. Fluorophore of smaller aromatic plane, such as 4-amino-7-nitro-2, 1,3-benzoxadiazole has also been shown as visible light excited fluorescent  $\text{Zn}^{2+}$  sensor [15]. The design and synthesis of fluorescent probes with high selectivity and sensitivity is a vibrant field of supramolecular chemistry for their fundamental role in medical, environmental and biological applications [16]. Although there are many fluorescent probes synthesized to detect zinc ion [16–18], there is none for ZnO nanoparticle; study on the fluorescence enhancement of bioactive imidazole derivatives [19] by ZnO nanoparticles has not been reported till now. And this is the first attempt of using imidazole derivative as a photosensor for ZnO nanoparticles. The highest occupied molecular orbital (HOMO) and lowest unoccupied molecular orbital (LUMO) potentials for the designed sensor must match with the conduction and valence band edges of the semiconductor nanocrystals. Quenching of fluorescence by various ligands, viz., phycoerythrin by  $\text{TiO}_2$ ,

C. Karunakaran · J. Jayabharathi (✉) · K. Brindha Devi ·  
K. Jayamoorthy  
Department of Chemistry, Annamalai University,  
Annamalainagar 608 002 Tamilnadu, India  
e-mail: jtchalam2005@yahoo.co.in

AuTiO<sub>2</sub> and AgTiO<sub>2</sub> [20], *meso*-tetraphenylporphyrin by TiO<sub>2</sub> [21], *meso*-tetrakis(4-sulfonatophenyl)porphyrins by TiO<sub>2</sub> [22], calf thymus-DNA by TiO<sub>2</sub> [23], porphyrins by TiO<sub>2</sub> [24] and CdS [25], phycocyanin by TiO<sub>2</sub> [25], bovine serum albumin by CdS [26] and TiO<sub>2</sub> [27], xanthine by CdS [28], polythiophene by TiO<sub>2</sub> [29] and bovine serum albumin by ZnO [30] have been reported. This is the first report of enhancement of fluorescence by ZnO nanoparticle. The observed fluorescence enhancement is unique to study the interaction between ZnO nanomaterial and imidazole derivative, to infer the association and also the energy transfer between them (Scheme 1). The imidazole-ZnO nanoparticle binding constant has been determined using the relationship  $(I-I_0)/I_0-[Q]$ . Scanning electron micrograph (SEM) and energy dispersive X-ray (EDX) spectrum confirms the adsorption of imidazole derivative on ZnO nanoparticle.

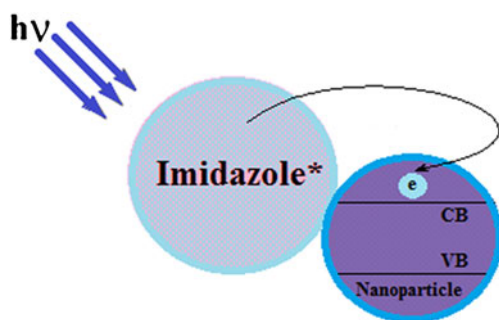
## Materials and Methods

### Materials

Benzil, cinnamaldehyde and all other reagents used were of analytical grade. The nanoparticulate ZnO used was that supplied by Sigma-Aldrich. It is of wurtzite structure with average crystallite size (*D*) and surface area (*S*) as 32 nm and 33 m<sup>2</sup> g<sup>-1</sup>, respectively [31].

### Synthesis of the 4,5-diphenyl-2(E)-styryl-1H-imidazole

The experimental procedure used was the same as described in our recent works [32–41]. The imidazole derivative was synthesized by three components assembling of benzil (40 mmol), ammonium acetate (30 mmol) and cinnamaldehyde (30 mmol). The three components were refluxed in ethanol for 24 h at 80 °C. The reaction mixture was extracted with dichloromethane and purified by column chromatography using hexane-ethyl acetate (9:1) as the eluent. Yield: 55 %. mp: 260 °C, Anal. calcd. for C<sub>23</sub>H<sub>18</sub>N<sub>2</sub>: C: 85.68; H: 5.63; N: 8.69. Found: C: 84.89; H: 5.23; N: 7.93. <sup>1</sup>H NMR



**Scheme 1** Photoinduced charge injection and charge separation

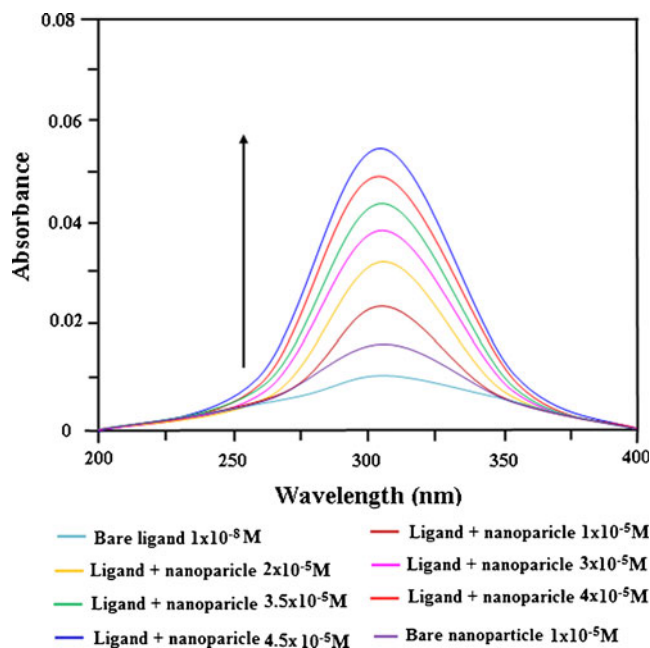


**Fig. 1** Absorption spectra of imidazole derivative in presence and absence of ZnO nanoparticle

(400 MHz, CDCl<sub>3</sub>): δ 9.87 (s, 1H), 8.09 (d, 1H), 8.01 (d, 1H), 7.98–6.79 (m, 15H). <sup>13</sup>C (100 MHz, CDCl<sub>3</sub>): δ 145.56, 136.48, 133.40–125.49 (Aromatic carbons). MS: m/e: obsd: 322.15, calcd: 321.68.

### Measurements

The <sup>1</sup>H and <sup>13</sup>C NMR spectra of the ligand were recorded on a Bruker 400 MHz NMR instrument and the mass spectrum was obtained using Agilent 1100 mass spectrometer. The fluorescence measurements were carried out with a Perkin Elmer LS55 spectrofluorimeter. The excitation wavelength was 305 nm and the emission was monitored at 380 nm. The excitation and emission slit width (each 10 nm) and scan rate (600 nm min<sup>-1</sup>) were kept unaltered for all the measurements. The sample was deoxygenated by bubbling with pure nitrogen gas. The absorption spectral measurements were recorded by using a Perkin Elmer Lambda 35 spectrophotometer. An



**Scheme 2** Electron-donating energy level of imidazole

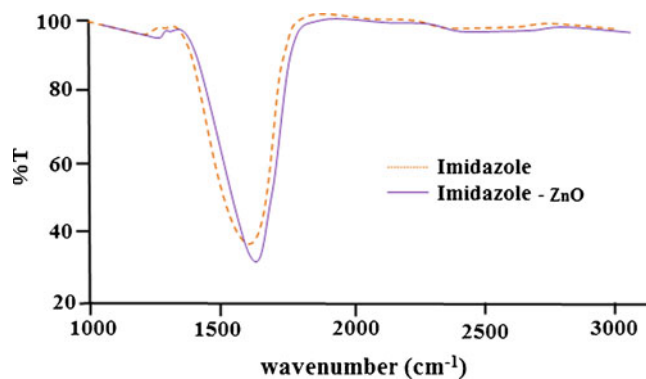


**Fig. 2** FT-IR spectra of imidazole (*broken line*) and imidazole bound with ZnO nanoparticulate (*solid line*)

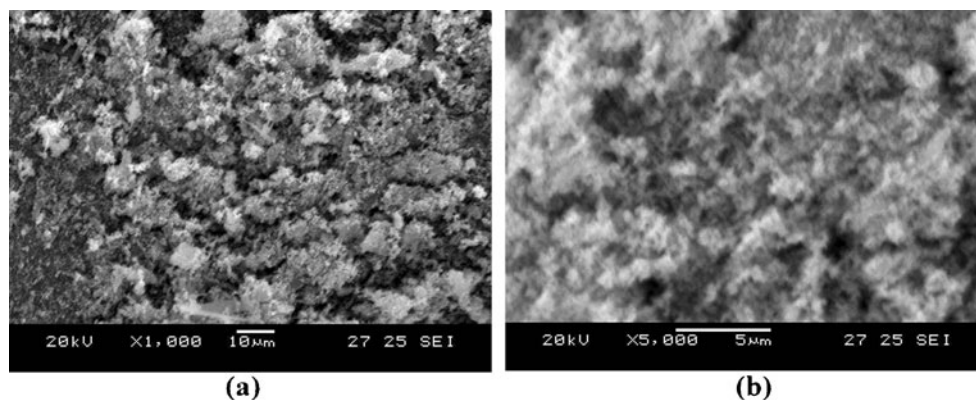
ethanolic solution of the imidazole derivative of required concentration ( $1 \times 10^{-8}$  M) was mixed with nanoparticles dispersed in ethanol at different loading and the absorbance and emission spectra were recorded. The nanocrystals were dispersed under sonication in ethanol using ethylene glycol followed by dilution with ethanol. The SEM and EDS spectra have been recorded by using JEOL-JSM 5610 LV.

## Results and Discussion

### Absorption Characteristics of Imidazole Derivative-ZnO Nanoparticle

The absorption spectra of the imidazole derivative in presence of ZnO nanoparticles dispersed at different loading and also in their absence are displayed in Fig. 1. The nanoparticles enhance the absorbance of imidazole derivative remarkably without shifting its absorption maximum at 305 nm. This indicates that the nanocrystals do not modify the excitation process of the ligand. The enhanced absorption at 305 nm observed with the dispersed semiconductor nanoparticle is due to adsorption of the imidazole derivative on semiconductor surface (Scheme 2). This is because of

**Fig. 3** **a** SEM image of ligand adsorbed ZnO nanoparticles. **b** SEM image of bare ZnO nanoparticle



effective transfer of electron from the excited state of the imidazole derivative to the conduction band of the semiconductor nanoparticle (PET mechanism).

### FT-IR Characteristics of Imidazole Derivative-ZnO Nanoparticle

The UV-visible absorption spectroscopy is not sufficient to throw light on the molecular structure of imidazole derivative adsorbed on surfaces of nanoparticles. Fourier transform infrared (FT-IR) technique may provide further information about the nature of interaction between the organic molecule and the ZnO surface. Fig. 2 shows the FT-IR spectrum of imidazole derivative (*broken line*) and imidazole derivative bound to the ZnO nanoparticle (*solid line*). The spectrum of pure imidazole derivative shows the  $>C=N$  stretching vibration at  $1596 \text{ cm}^{-1}$ . This band is shifted from  $1596 \text{ cm}^{-1}$  to  $1633 \text{ cm}^{-1}$  for imidazole derivative bound to the ZnO nanoparticle. This confirms that the imidazole derivative is adsorbed on the surface of the ZnO nanoparticle.

### Scanning Electron Micrograph (SEM) and Energy Dispersive Spectrum (EDS)

Figure 3 presents the scanning electron micrographs of imidazole derivative adsorbed ZnO nanoparticles and bare ZnO nanocrystal. The SEM images show that imidazole adsorption does not significantly modify the morphology of the ZnO nanocrystal. The EDS (Fig. 4) of the imidazole treated ZnO nanoparticle and bare ZnO nanocrystal confirm the adsorption of imidazole derivative on ZnO nanocrystal-line surface.

### Fluorescence Enhancement

The emission spectra of imidazole derivative in presence of ZnO nanoparticle dispersed at different loading and also in their absence are displayed in Fig. 5. The nanoparticle enhances the emission of imidazole derivative remarkably

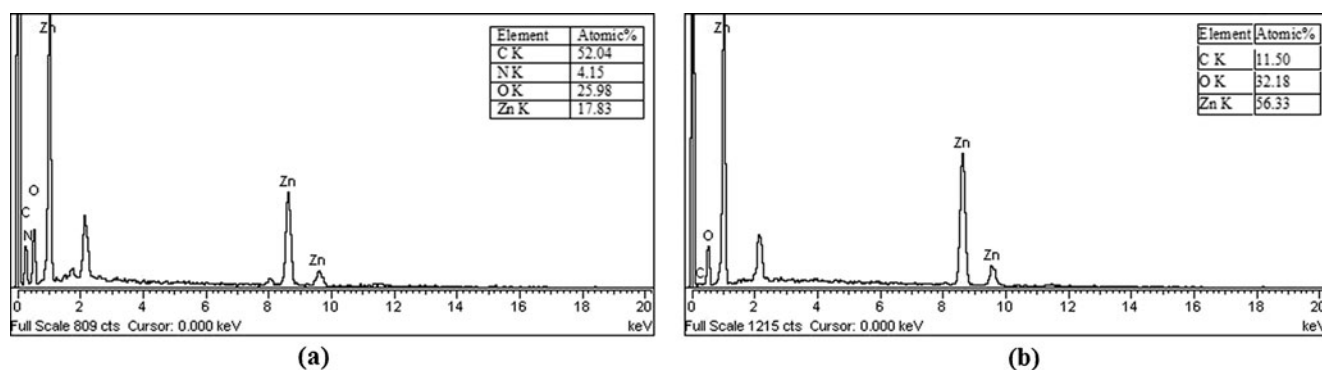


**Fig. 4** **a** EDX spectra of ligand adsorbed ZnO nanoparticle. **b** EDX spectra of bare ZnO nanoparticle

without shifting its emission maximum at 380 nm. This indicates that the nanocrystal do not modify the excitation process of the ligand. The enhanced emission at 380 nm observed with the dispersed semiconductor nanoparticle is due to the adsorption of the imidazole derivative on semiconductor surface. This is because of effective transfer of electron from the excited state of the imidazole derivative to the conduction band of the semiconductor nanoparticle. Fluorescence enhancement arises due to formation of complex the fluorophore–nanoparticulate ZnO and the binding constant ( $K$ ) has been calculated as  $1.240 \times 10^3$ .

#### Energetics

From the onset oxidation potential ( $E_{ox}$ ) and the onset reduction potential ( $E_{red}$ ) of the imidazole derivative,

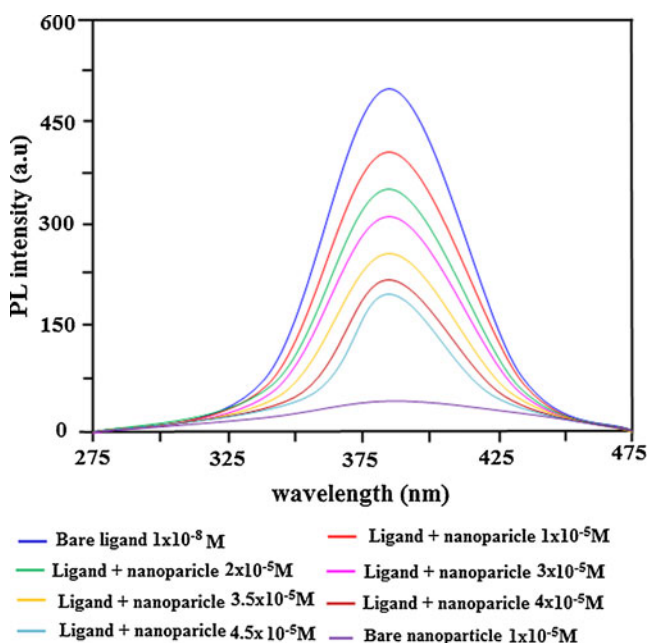


**Fig. 5** Fluorescence enhancement of imidazole derivative in the presence and absence of various concentrations of ZnO nanoparticle

HOMO and LUMO energy levels have been calculated according to the following equations [42]:

$$\text{HOMO} = -e(E_{ox} + 4.71) \text{ (eV)} \quad (1)$$

$$\text{LUMO} = -e(E_{red} + 4.71) \text{ (eV)} \quad (2)$$

On the basis of the relative positions of imidazole derivative and ZnO energy levels shown in Fig. 6, the electron injection would be thermodynamically allowed from the excited singlet of the imidazole derivative to the conduction band of ZnO.

Figure 6 presents the HOMO and LUMO energy levels of an isolated imidazole molecule along with the conduction band and valence band edges of ZnO

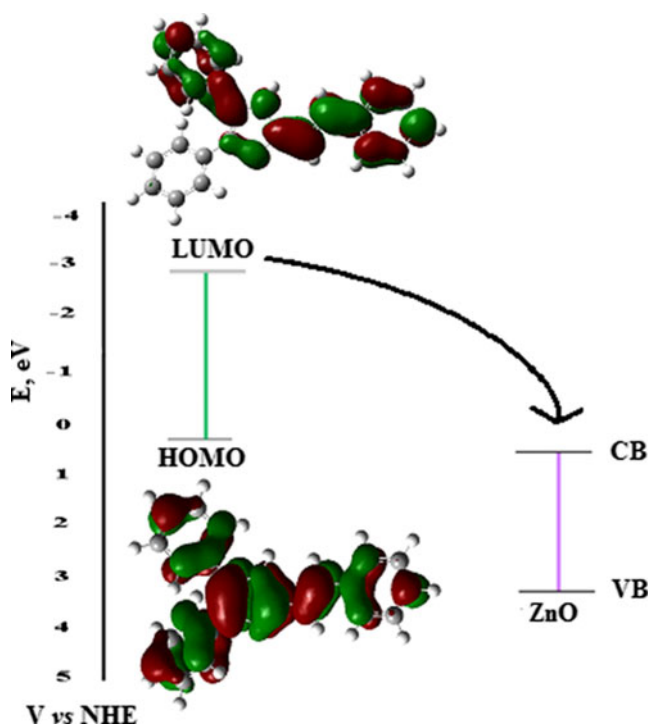


**Fig. 6** Electron-donating energy level of imidazole

nanoparticle. The energy levels presented in Fig. 7 suggests enhancement of fluorescence of imidazole derivative by ZnO nanocrystal. On illumination at 305 nm both the ligand and nano semiconductor are excited. Dual emission is expected due to LUMO→HOMO and CB→VB electron transfer. Also possible is electron jump from the excited ligand to the nanocrystal; the electron in the LUMO of the excited ligand is of higher energy compared to that in the CB of ZnO nanocrystals. This should lead to quenching of fluorescence of imidazole derivative. However, contrary to the expectations, enhancement of fluorescence is observed in presence of ZnO nanocrystal. This may be because of the lowering of the HOMO and LUMO energy levels of imidazole derivative due to adsorption on ZnO nanoparticle. The polar ZnO surface enhances the delocalisation of the π electrons and lowers the HOMO and LUMO energy levels due to adsorption [43]. The chemical affinity between the nitrogen atom of the imidazole and zinc ion on the surface of the nano oxide may be a reason for strong adsorption of the ligand on nanoparticle causes the enhancement (Fig. 8).

The excited state energy of the imidazole derivative, as shown in Scheme 2, is larger than the conductance band energy levels of nanosemiconductors [44]. This makes possible the energy transfer from the excited state of imidazole derivative to the nanoparticle.

According to Forster’s energy transfer theory, the energy transfer efficiency is related not only to the distance between

### Mechanism of Enhancement

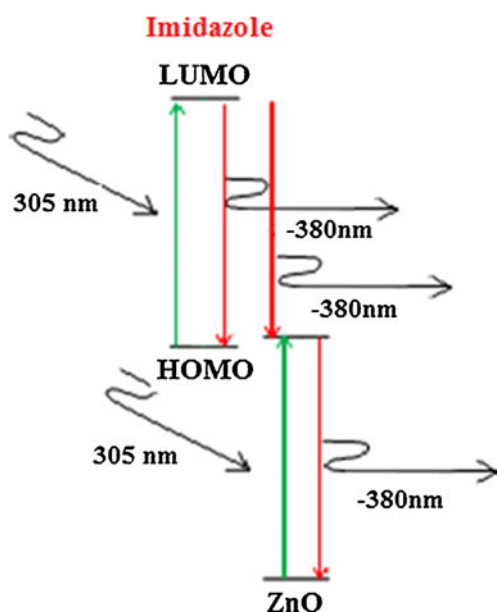


Fig. 7 Chemical bonding interaction of imidazole derivative with ZnO nanoparticle

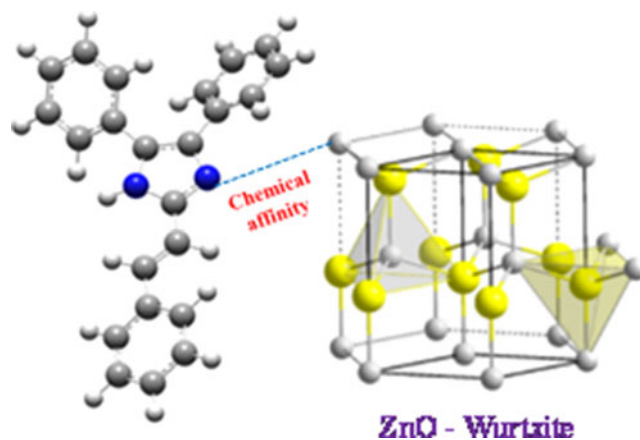


Fig. 8 Chemical affinity between the nitrogen atom of the imidazole and zinc ion on the surface of the nano oxide

the acceptor and donor ( $r_0$ ), but also to the critical energy transfer distance ( $R_0$ ). That is

$$E = R^6_0 / (R^6_0 + r^6_0) \tag{3}$$

where,  $R_0$  is the critical distance when the transfer efficiency is 50 %.

$$R^6_0 = 8.8 \times 10^{-25} K^2 N^{-4} \phi J \tag{4}$$

where,  $K^2$  is the spatial orientation factor of the dipole,  $N$  is the refractive index of the medium,  $\phi$  is the fluorescence quantum yield of the donor and  $J$  is the overlap integral of the fluorescence emission spectrum of the donor and the absorption spectrum of the acceptor (Fig. 9). The value of  $J$  can be calculated by using Eq. (5),

$$J = \int F(\lambda)\epsilon(\lambda)\lambda^4 d\lambda / \int F(\lambda) d\lambda \tag{5}$$

where,  $F(\lambda)$  is the fluorescence intensity of the donor,  $\epsilon(\lambda)$  is molar absorptivity of the acceptor. The parameter  $J=0.84$

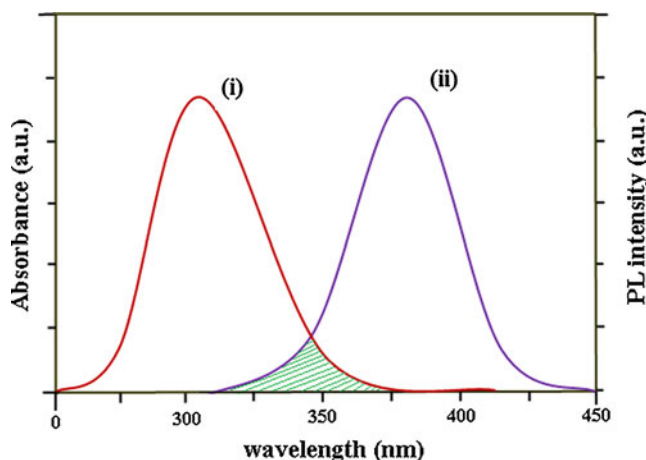


Fig. 9 Overlapping of fluorescence and absorption spectra of donor and acceptor

$10^9 \text{ J (cm}^3 \text{ M}^{-1})$  evaluated by integrating the spectral parameters in Eq. (5). Under these experimental conditions, the value of  $E$ ,  $R_0$  and  $r_0$  calculated was found to be about 0.228, 1.71 and 2.09 nm in all cases; the values of  $K^2$  ( $= 2/3$ ) and  $N$  ( $= 1.3467$ ) used are from the literature [45] and the  $\varphi$  value ( $= 0.15$ ) is from the present study. Obviously, the calculated value of  $R_0$  is in the range of maximal critical distance. This is in accordance with the conditions of Forster's energy transfer theory [46], suggests that energy transfer occurs between the ZnO nanoparticle and imidazole derivative with high probability [47].

#### Free-Energy Change ( $\Delta G_{et}$ ) for Electron Transfer Process

The thermodynamic feasibility of excited state electron transfer reaction has been confirmed by the calculation of free energy change by employing the well known Rehm-Weller expression [48].

$$\Delta G_{et} = E^{1/2}_{(ox)} - E^{1/2}_{(red)} - E_s + C \quad (6)$$

where,  $E_{(ox)}^{1/2}$  is the oxidation potential of imidazole derivative (0.14 V),  $E_{(red)}^{1/2}$  is the reduction potential of ZnO nanoparticle, i.e., the conduction band potential of nanoparticle,  $E_s$  is the excited state energy of imidazole derivative and  $C$  is the coulombic term. Since the ligand is neutral and the solvent used is polar in nature, the coulombic term in the above expression can be neglected [49]. The values of  $\Delta G_{et}$  is calculated as  $-2.80 \text{ eV}$ . The high negative values indicate the thermodynamic feasibility of the electron transfer process [50–54].

#### Conclusion

Imidazole derivative is adsorbed on the surface of semiconductor nanoparticle through azomethine nitrogen. The conduction band energy position determines the electron transfer from excited state imidazole derivative to the ZnO nanoparticles. Based on photo-induced electron transfer (PET) mechanism, fluorescent enhancement has been explained and apparent binding constant has been calculated. The negative  $\Delta G_{et}$  value for ZnO nanoparticles reveals that the electron transfer process is thermodynamically favourable.

**Acknowledgment** One of the authors Dr. J. Jayabharathi, Associate Professor, Department of Chemistry, Annamalai University is thankful to Department of Science and Technology [No. SR/S1/IC-73/2010] and University Grants Commission [F. No. 36-21/2008 (SR)] for providing funds for this research study.

#### References

- Colvin VL, Schlamp MC, Alivisatos AP (1994) Light-emitting diodes made from cadmium selenide nanocrystals and a semiconducting polymer. *Nature* 370:354–357
- Moller BM, Woggon U, Artemyev MV (2005) Coupled-resonator optical waveguides doped with nanocrystals. *Opt Lett* 30:2116–2118
- Bruchez M, Moronne M, Gin P, Weiss S, Alivisatos AP (1998) Semiconductor nanocrystals as fluorescent biological labels. *Science* 281:2013–2016
- Wu X, Liu H, Liu J, Haley K, Treadway J, Larson J, Ge N, Peals F, Bruchez M (2002) Immunofluorescent labeling of cancer marker Her2 and other cellular targets with semiconductor quantum dots. *Nat Biotechnol* 21:41–46
- Gao X, Cui Y, Levenson RM, Chung L, Nie S (2004) In vivo cancer targeting and imaging with semiconductor quantum dots. *Nat Biotechnol* 22:969–976
- Bravner R, Ferrari-Iliou R, Brivois N, Djediat S, Benedetti MF, Fievet F (2006) Toxicological impact studies based on *Escherichia coli* bacteria in ultrafine ZnO nanoparticles colloidal medium. *NanoLett* 6:866–870
- Wang X, Kong X, Yu Y, Zhang H (2007) Semiconductor nanocrystals as fluorescent biological labels. *J Phys Chem C* 111:3836–3841
- Hu W, Liu Y, Yang H, Zhou X, Li CM (2011) ZnO nanorods-enhanced fluorescence for sensitive microarray detection of cancers in serum without additional reporter-amplification. *Biosens Bioelectron* 26:3683–3687
- Lefebvre JF, Leclercq D, Gisselbrecht JP, Richeter S (2010) Synthesis, characterization, and electronic properties of metalloporphyrins annulated to exocyclic imidazole and imidazolium rings. *Eur J Org Chem* 2010:1912–1920
- Shi L, Su J, Wu Z (2011) First-principles studies on the efficient photoluminescent iridium(III) complexes with C<sup>N</sup>=N ligands. *Inorg Chem* 50:5477–5484
- Adachi M, Nagao M (2001) Design of near-infrared dyes Based on  $\pi$ -conjugation system extension 2. Theoretical elucidation of framework extended derivatives of perylene chromophore. *Chem Mater* 13:662–669
- Yan YN, Pan YL, Song HC (2010) The synthesis and optical properties of novel 1,3,4-oxadiazole derivatives containing an imidazole unit. *Dyes Pigments* 86:249–258
- Que EL, Domaille DW, Chang CJ (2008) Metals in neurobiology: probing their chemistry and biology with molecular imaging. *Chem Rev* 108:1517–1549
- Komatsu K, Urano Y, Kojima H, Nagano T (2007) Development of an iminocoumarin-based zinc sensor suitable for ratiometric fluorescence imaging of neuronal zinc. *J Am Chem Soc* 129:13447–13454
- Qian F, Zhang C, Zhang Y, He W, Gao X, Hu P, Guo Z (2009) Visible light excitable Zn(2+) fluorescent sensor derived from an intramolecular charge transfer fluorophore and its in vitro and in vivo application. *J Am Chem Soc* 131:1460–1468
- Li Z, Yu M, Zhang L, Yu M, Liu J, Wei L, Zhang H (2010) A “switching on” fluorescent chemodosimeter of selectivity to Zn<sup>2+</sup> and its application to MCF-7 cells. *Chem Commun* 46:7169–7171
- Xu Z, Baek KH, Kim HN, Cui J, Qian X, Spring DR, Shin I, Yoon J (2010) Zn<sup>2+</sup>-triggered amide tautomerization produces a highly Zn<sup>2+</sup>-selective, cell-permeable, and ratiometric fluorescent sensor. *J Am Chem Soc* 132:601–610
- Moon WJ, Yu JH, Choi GM (2001) Selective CO gas detection of SnO<sub>2</sub>-Zn<sub>2</sub>SnO<sub>4</sub> composite gas sensor. *Sensor Actuator B* 80:21–27
- Jayabharathi J, Thanikachalam V, Saravanan K, Srinivasan N (2011) Iridium(III) complexes with orthometalated phenylimidazole ligands

- subtle turning of emission to the saturated green colour. *J Fluoresc* 21:507–519
20. Kathiravan A, Chandramohan M, Renganathan R, Sekar S (2009) Photoinduced electron transfer from phycoerythrin to colloidal metal semiconductor nanoparticles. *Spectrochim Acta A* 72:496–501
  21. Kathiravan A, Renganathan R (2008) An investigation on electron transfer quenching of zinc(II) *meso*-tetraphenylporphyrin (ZnTPP) by colloidal TiO<sub>2</sub>. *Spectrochim Acta A* 71:1106–1109
  22. Kathiravan A, Anbazhagan V, Asha Jhonsi M, Renganathan R (2008) Fluorescence quenching of *meso*-tetrakis(4-sulfonatophenyl)porphyrins by colloidal TiO<sub>2</sub>. *Spectrochim Acta A* 70:615–618
  23. Kathiravan A, Renganathan R (2009) Photoinduced interactions between colloidal TiO<sub>2</sub> nanoparticles and calf thymus-DNA. *Polyhedron* 28:1374–1378
  24. Kathiravan A, Renganathan R (2009) Effect of anchoring group on the photosensitization of colloidal TiO<sub>2</sub> nanoparticles with porphyrins. *J Colloid Interface Sci* 331:401–407
  25. Asha Jhonsi M, Kathiravan A, Renganathan R (2009) An investigation on fluorescence quenching of certain porphyrins by colloidal CdS. *J Lumin* 129:854–860
  26. Asha Jhonsi M, Kathiravan A, Renganathan R (2009) Spectroscopic studies on the interaction of colloidal capped CdS nanoparticles with bovine serum albumin. *Colloid Surface B* 72:167–172
  27. Kathiravan A, Renganathan R (2008) Interaction of colloidal TiO<sub>2</sub> with bovine serum albumin: a fluorescence quenching study. *Colloid Surface A* 324:176–180
  28. Asha Jhonsi M, Kathiravan A, Renganathan R (2009) Photoinduced interaction between xanthenes dyes and colloidal CdS nanoparticles. *J Mol Struct* 921:279–284
  29. Chen JM, Hou JH, Li YF, Zhou XW, Zhang JB, Li XP, Xiao XR, Lin Y (2009) Fluorescence and sensitization performance of phenylene-vinylene-substituted polythiophene. *Chin Sci Bull* 54:1669–1676
  30. Kathiravan A, Paramaguru G, Renganathan R (2009) Study on the binding of colloidal zinc oxide nanoparticle with bovine serum albumin. *J Mol Struct* 921:279–284
  31. Karunakaran C, Anilkumar P, Gomathisankar P (2011) Photoproduction of iodine with nanoparticulate semiconductors and insulators. *Chem Cent J* 123:5–31
  32. Gayathri P, Jayabharathi J, Srinivasan N, Thiruvalluvar A, Butcher RJ (2010) 2-(4-Fluorophenyl)-1,4,5-triphenyl-1*H*-imidazole. *Acta Crystallogr E* 66:o1703
  33. Jayabharathi J, Thanikachalam V, Venkatesh Perumal M, Saravanan K (2011) Displacement reaction using ibuprofen in a mixture of bioactive imidazole derivative and bovine serum albumin—a fluorescence quenching study. *J Fluoresc*. doi:10.1007/s10895-011-0878-3
  34. Jayabharathi J, Thanikachalam V, Venkatesh Perumal M, Srinivasan N (2011) Fluorescence resonance energy transfer from a bio-active imidazole derivative 2-(1-phenyl-1*H*-imidazo[4,5-*f*][1,10]phenanthroline-2-yl)phenol to a bioactive indoloquinolizine system. *Spectrochim Acta A* 79:236–244
  35. Jayabharathi J, Thanikachalam V, Saravanan K, Srinivasan N, Venkatesh Perumal M (2011) Physicochemical properties of organic nonlinear optical crystal from combined experimental and theoretical studies. *Spectrochim Acta A* 78:794–802
  36. Jayabharathi J, Thanikachalam V, Jayamoorthy K, Venkatesh Perumal M (2011) A physicochemical study of excited state intramolecular proton transfer process: luminescent chemosensor by spectroscopic investigation supported by *ab initio* calculations. *Spectrochim Acta A* 79:6–16
  37. Jayabharathi J, Thanikachalam V, Srinivasan N, Jayamoorthy K, Venkatesh Perumal M (2011) An intramolecular charge transfer fluorescent probe: synthesis, structure and selective fluorescent sensing of Cu<sup>2+</sup>. *J Fluoresc* 21:1813–1823
  38. Jayabharathi J, Thanikachalam V, Saravanan K (2009) Effect of substituents on the photoluminescence performance of Ir(III) complexes: synthesis, electrochemistry and photophysical properties. *J Photochem Photobiol A Chem* 208:13–20
  39. Jayabharathi J, Thanikachalam V, Brindha Devi K, Venkatesh Perumal M (2011) Binding interaction of bioactive imidazole with bovine serum albumin—A mechanistic investigation. *Spectrochim Acta A*. doi:10.1016/j.saa.2011.08.081
  40. Jayabharathi J, Thanikachalam V, Brindha Devi K, Srinivasan N (2011) Physicochemical studies of some novel Y-shaped imidazole derivatives—a sensitive chemisensor. *Spectrochim Acta A* 82:513–520
  41. Saravanan K, Srinivasan N, Thanikachalam V, Jayabharathi J (2010) Synthesis and photophysics of some novel imidazole derivatives used as sensitive fluorescent chemisensors. *J Fluoresc* 21:65–80
  42. Hou J, Huo L, He C et al (2006) Synthesis and absorption spectra of poly(3-phenylenevinyl)thiophene with conjugated side chains. *Macromolecules* 39(2):594–603
  43. Cheng HM, Hsieh WF (2010) Electron transfer properties of organic dye-sensitized solar cells based on indoline sensitizers with ZnO nanoparticles. *Nanotech* 21:485202
  44. Lin B, Fu Z, Ji Y (1991) Green luminescent center in undoped zinc oxide films deposited on silicon substrates. *Appl Phys Lett* 79:943–945
  45. Cyril L, Earl JK, Sperry WM (196) *Biochemists' handbook*. E. & F. N. Spon, London, pp 84–88
  46. Chen GZ, Huang XZ, Xu JG, Wang ZB, Zheng ZZ (1990) *Method of fluorescent analysis* (chapter 4), 2nd edn. Science Press, Beijing, p 126
  47. He WY, Li Y, Xue CX, Hu ZD, Chen XG, Sheng FL (2005) Effect of Chinese medicine alpinetin on the structure of human serum albumin. *Bioorg Med Chem* 13:1837–1845
  48. Kavarnos GJ, Turro NJ (1986) Photosensitization by reversible electron transfer: theories, experimental evidence, and examples. *Chem Rev* 86:401–449
  49. Parret S, Savary FM, Fouassier JP, Ramamurthy P (1994) Spin-orbit-coupling-induced triplet formation of triphenylpyrylium ion: a flash photolysis study. *J Photochem Photobiol A* 83:205–209
  50. Kikuchi K, Niwa T, Takahashi Y, Ikeda H, Miyashi T (1993) Quenching mechanism in a highly exothermic region of the Rehm-Weller relationship for electron-transfer fluorescence quenching. *J Phys Chem* 97:5070–5073
  51. Nath S, Pal H, Palit DK, Sapre AV, Mittal JP (1998) Steady-state and time-resolved studies on photoinduced interaction of phenothiazine and 10-methylphenothiazine with chloroalkanes. *J Phys Chem A* 102:5822–5830
  52. Domenech J, Prieto A (1986) Stability of ZnO particles in aqueous suspensions under UV illumination. *J Phys Chem* 90:1123–1126
  53. Joshi C, Kumar K, Rai SB (2011) Effect of ZnO as modifier on up and downconversion properties of Ho<sup>3+</sup>/Yb<sup>3+</sup> doped tellurite glasses. *Opt Commun* 284:4584–4587
  54. Kathiravan A, Renganathan R (2009) Photosensitization of colloidal TiO<sub>2</sub> nanoparticles with phycocyanin pigment. *J Colloid Interface Sci* 335:196–202